

COMPUTER-AIDED DESIGN OF Y-JUNCTION WAVEGUIDE DIPLEXERS

F. M. Vanin [†] and F. Frezza

Department of Information Engineering, Electronics, and
Telecommunications
La Sapienza University of Rome
Via Eudossiana 18, Roma 00184, Italy

D. Schmitt

European Space Agency — European Space Research and
Technology Centre (ESA-ESTEC)
Keplerlaan 1, 2201AZ Noordwijk, The Netherlands

Abstract—Waveguide diplexer designs are widely used for telecommunications, space, and terrestrial applications. Although mathematical models and design procedures for waveguide filters are known, diplexer designs still remain complex and time consuming. This paper describes how to obtain an equivalent circuit network model and a complete design of non-contiguous diplexers using a computer-aided approach with a classic Y-junction. Results are satisfactory in terms of reduced design time and performance. Examples including physical dimensions are provided.

1. INTRODUCTION

Diplexers are used in a large variety of applications in communication systems. They typically follow the antenna in the RF chain allowing simultaneously transmit and receive functions. A diplexer is a device that splits a signal into two groups according to predefined frequency ranges, or combines two signals, each occupying a separate frequency range, into a single collection of signals. Diplexers subdivide a wide frequency band in two narrower bands or, reciprocally, combine

Received 20 September 2010, Accepted 2 November 2010, Scheduled 12 November 2010
Corresponding author: Felice Maria Vanin (felice.vanin@esa.int).

[†] Also with European Space Agency — European Space Research and Technology Centre (ESA-ESTEC), Keplerlaan 1, 2201AZ Noordwijk, The Netherlands.

frequency bands into a common port. There are mainly two types of diplexer, contiguous and non-contiguous ones. In a non-contiguous diplexer, the bands of the filters are separated in frequency with a frequency separation called ‘guardband’ whereas, in the contiguous case, the bands are adjacent.

This paper focuses on diplexers realized in rectangular waveguides connecting two inductive iris bandpass filters. The design typically starts with the establishment of the main RF specifications, e.g., Transmit/Receive frequency ranges, insertion loss variation, return loss, and rejection at Transmit/Receive bands. Each filter is then modelled and physical dimensions calculated i.e., waveguide lengths and iris dimensions. Subsequently, the filters are combined at the common port. This connection can be done, for example, with N-furcation, T-junctions, or Y-junction. In this article, the Y-junction is chosen as connection between the two filters. The connection of the two filters at the common port requires typically optimization loops of the entire structure. To ease the dimensional design process in terms of time and complexity, excessive use of optimisation should be prevented, especially in diplexer structures where there are numerous dimensions to be optimised.

Accurate transfer functions for calculating network models of bandpass filters and diplexers are known and published for example in [1–3]. In addition information on how to derive physical dimensions of bandpass filters and diplexers is also provided in [4] and [5] but without indicating how diplexer circuit models can be calculated.

The aim of this work is to provide practical formulas to derive a Y-junction diplexer network model (see Figure 1) giving examples of diplexer network synthesis, including physical dimensions and fullwave analyses. A FORTRAN software code has been written to assist engineers in the design of diplexers limiting the optimization variables following an automatic and systematic approach as indicated in [5]. This prevents the use of common techniques requiring time-consuming global fullwave optimization. The FORTRAN programming language was chosen due to its accurate numerical computation, speed, and portability with respect to operative system.

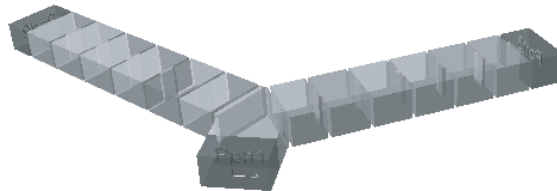


Figure 1. 3D cad drawing of a diplexer.

2. MATHEMATICAL MODEL

2.1. Diplexer Admittance Matrix

The object of this section is to provide formulas to be used in the definition of a diplexers network model.

Since a diplexer is a three port device, it can be modeled using a 3×3 either admittance or impedance matrix. Figure 2 indicates the block diagram of a diplexer network model, where the junction is represented by the admittance matrix Y , and the two filters by the admittance matrices Y^{F1} and Y^{F2} .

The matrix Y can be written as:

$$Y = \begin{pmatrix} Y_{11} & Y_{12} & Y_{13} \\ Y_{21} & Y_{22} & Y_{23} \\ Y_{31} & Y_{32} & Y_{33} \end{pmatrix} \tag{1}$$

while the two admittance filter matrices Y^{F1} and Y^{F2} :

$$\begin{cases} Y^{F1} = \begin{pmatrix} Y_{11}^{F1} & Y_{21}^{F1} \\ Y_{21}^{F1} & Y_{22}^{F1} \end{pmatrix} \\ Y^{F2} = \begin{pmatrix} Y_{11}^{F2} & Y_{21}^{F2} \\ Y_{21}^{F2} & Y_{22}^{F2} \end{pmatrix} \end{cases} \tag{2}$$

Considering the voltages V_1, V_2, V_3 and currents I_1, I_2, I_3 respectively at port 1, 2, 3, the following can be written:

$$\begin{pmatrix} I_1 \\ I_2 \\ I_3 \end{pmatrix} = Y^{Dip} \cdot \begin{pmatrix} V_1 \\ V_2 \\ V_3 \end{pmatrix} \tag{3}$$

Using the network in Figure 2, the Kirchoff equations can be written and solved in Y^{Dip} in terms of Y^{F1} and Y^{F2} :

$$Y^{Dip} = \begin{pmatrix} Y_{11}^{Dip} & Y_{12}^{Dip} & Y_{13}^{Dip} \\ Y_{21}^{Dip} & Y_{22}^{Dip} & Y_{23}^{Dip} \\ Y_{31}^{Dip} & Y_{32}^{Dip} & Y_{33}^{Dip} \end{pmatrix} \tag{4}$$

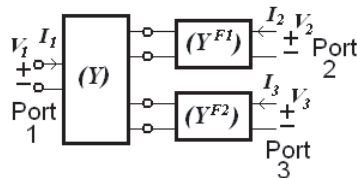


Figure 2. Diplexer network model.

Note that the network can be solved also in terms of the impedance matrix rather than the admittance matrix (clearly both models are electrically equivalent).

The complete analytical expression for matrix (4) is given in the Appendix (the case of Z matrix representation is also provided). The explicit expression of Y^{Dip} can be used to create a mathematical model of the Diplexer. Such equations are independent of the practical realization of the junction and therefore are still valid for junctions different from the Y-junction.

2.2. Y-Junction and Filter Admittance Matrices

In order to complete the analytical model of the diplexer, explicit expressions for the matrices Y^{F1} , Y^{F2} , and Y are necessary. The objective is to show how to calculate those matrices and to derive consequently a diplexer response. It is first indicated how to calculate the junction admittance matrix and then the filter admittance matrices.

Since lumped element models for the junction typically do not include the frequency dependence of waveguide structures (unless advanced models are used), it is preferred to use standard fullwave simulators to derive accurate results. With the use of a fullwave simulator (in our case [9]), it is possible to calculate the S matrix response of a Y-junction in the frequency range of interest. The S matrix can be then converted in Y matrix just using analytical matrix transformations.

This way of proceeding ensures a very accurate model of the Y-junction which includes the frequency dependency of the junction structure. The Y admittance matrix of the junction is then calculated.

In order to calculate the filter admittance matrices Y^{F1} and Y^{F2} , it is necessary to choose the filter network model. Typically, waveguide bandpass filters exhibiting Chebychev characteristics are represented either with coupling matrices [6] or with a model based on impedance inverters cascaded with transmission lines as indicated in [1, 5]. In this article the model is chosen based on impedance inverters which give a direct link between network characteristics and physical model as indicated in Figure 3.

A possible realization in rectangular waveguide of a Chebychev bandpass filter is composed of a cascade of resonators separated by inductive irises. Figure 3(a) contains a schematic of a 4-pole filter and the equivalent network model based on a cascade of impedance inverters and transmission lines with characteristic impedance Z_0 . The widths of irises, represented by a frequency independent impedance

inverter K_{ij} , are denoted as W_1, W_2, W_3 , and the letters R_1, R_2 indicate the resonator lengths, represented by transmission lines. Thus, the geometrical structure is mapped into a network model. To be noted that this circuit model clearly simplifies the actual behavior of waveguides: for example, it does not include higher order modes and the frequency dependence of the coupling elements. In any case, the model given in Figure 3(b) is a good approximation of a waveguide filter when these effects can be ignored, namely for narrow bandwidth (BW) applications.

The filter network model is completed when the values of the impedance inverters, the resonator lengths, and the characteristic impedance of the line have been determined.

We assume that all resonators are tuned to the same centre frequency $f_0 = BW/2$ and therefore, in the network model, the lengths of the resonators (i.e., of the transmission lines) are identical and given by:

$$l = m \frac{\lambda_{g0}}{2} \quad m = 1, 2, \dots \tag{5}$$

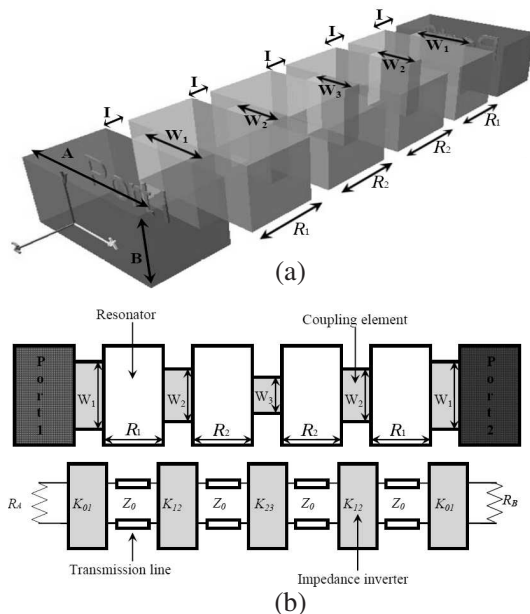


Figure 3. (a) 3D drawing of a 4-pole bandpass filter in rectangular waveguide. (b) Top-view of a bandpass filter in rectangular waveguide and its network model.

where λ_{g0} is the guide-wavelength at the centre frequency, and m the number of half wavelengths. For the example, the TE_{101} mode has been selected and therefore the value for m is 1.

The remaining network model parameters are Z_0 and K_{ij} . The characteristic impedance Z_0 can be set to any real value. For simplicity we choose the value of $Z_0 = 1 \Omega$.

For a given filter degree n of fractional bandwidth $w = BW/f_0$, the impedance inverters are defined as given in [6]:

$$\begin{cases} K_{01} = k_{01}\sqrt{R_A \cdot x \cdot w} \\ K_{j,j+1}|_{j=1,n-1} = w \cdot x \cdot k_{j,j+1} \\ K_{n,n+1} = k_{n,n+1}\sqrt{R_B \cdot x \cdot w} \end{cases} \quad (6)$$

where the normalised coupling elements $k_{j,j+1}$ are calculated from the lowpass prototype elements defined in [6] for Chebychev filters by the following:

$$k_{i,i+1}|_{i=0,\dots,n} = \frac{1}{\sqrt{g_i g_{i+1}}} \quad (7)$$

In Equation (6), R_A and R_B are the resistances which close the line on the left- and right-hand side of the network in Figure 3(b). These resistances are the normalising elements for calculating the S -parameters and usually taken to the value of Z_0 (i.e., in this case, both equal to 1). x is the reactance slope parameter of the series resonator given by:

$$x = \frac{\pi}{2} Z_0 \left(\frac{\lambda_{g0}}{\lambda_0} \right)^2 \quad (8)$$

where λ_0 is the wavelength at the centre frequency f_0 .

Having dimensioned all network elements, the filter model is completed. In general, for an n -pole filter, the transfer matrix T_{ij} is obtained by multiplying the transfer matrix elements of the circuit as follows:

$$\begin{aligned} \begin{pmatrix} T_{11} & T_{12} \\ T_{21} & T_{22} \end{pmatrix} &= \begin{pmatrix} \cos(\beta L) & jZ_0 \sin(\beta L) \\ \frac{j}{Z_0} \sin(\beta L) & \cos(\beta L) \end{pmatrix} \cdot \begin{pmatrix} 0 & iK_{01} \\ \frac{i}{K_{01}} & 0 \end{pmatrix} \\ &\cdot \begin{pmatrix} \cos\left(\pi \frac{\lambda_{g0}}{\lambda_g}\right) & iZ_0 \sin\left(\pi \frac{\lambda_{g0}}{\lambda_g}\right) \\ \frac{i \sin\left(\pi \frac{\lambda_{g0}}{\lambda_g}\right)}{Z_0} & \cos\left(\pi \frac{\lambda_{g0}}{\lambda_g}\right) \end{pmatrix} \cdot \begin{pmatrix} 0 & iK_{12} \\ \frac{i}{K_{12}} & 0 \end{pmatrix} \\ &\cdots \begin{pmatrix} \cos\left(\pi \frac{\lambda_{g0}}{\lambda_g}\right) & iZ_0 \sin\left(\pi \frac{\lambda_{g0}}{\lambda_g}\right) \\ \frac{i \sin\left(\pi \frac{\lambda_{g0}}{\lambda_g}\right)}{Z_0} & \cos\left(\pi \frac{\lambda_{g0}}{\lambda_g}\right) \end{pmatrix} \cdot \begin{pmatrix} 0 & iK_{n+1} \\ \frac{i}{K_{n+1}} & 0 \end{pmatrix} \quad (9) \end{aligned}$$

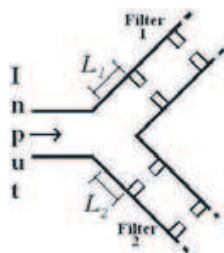


Figure 4. Connection of the filters to the Y-junction, detail of L_1 and L_2 .

Note that in Equation (9), a transmission line of length L is positioned at the left side of the first coupling representing the waveguide connecting the filter to the common junction. In order to ensure adequate electrical matching between the filters and the junction, the lengths L_1 and L_2 respectively connecting filter 1 and 2 to the common port have to be appropriately chosen, as indicated in Figure 4.

An analytical solution to calculate L_1 and L_2 is possible as indicated in [8] using the phase information for the two filters and the scattering parameters characterizing the junction. For convenience, the formulas, (A3) and (A4), are provided in the appendix.

After calculating L_1 and L_2 , Equation (9) can be finally transformed into the admittance matrices Y^{F1} and Y^{F2} with the simple use of network formulas.

Using now the three matrices Y , Y^{F1} , and Y^{F2} , Y^{Dip} can be calculated using the formula (A1) given in the appendix. The S matrix can be then derived using:

$$S = (I + Y^{Dip})^{-1} (I - Y^{Dip}) \quad (10)$$

3. SUMMARY OF THE NETWORK DESIGN PROCEDURE AND EXAMPLES

A FORTRAN code has been written including all the equations previously described. In this section, a digest of the diplexer design procedure is given including 2 examples.

The network diplexer synthesis proceeds as follows:

- 1) The waveguide type for the Y-junction and the filters shall be selected according to the working frequency range, and a suitable iris thickness chosen.
- 2) The Y-junction shall be analysed with a fullwave simulator to calculate S -parameters and then convert them into the Y matrix.

- 3) In accordance with Figure 3(b) and with the RF specifications, the network models of the filters shall be calculated: the impedance inverters using (6), and the resonator lengths using (5).
- 4) The transfer matrix T_{ij} of the filters shall be calculated using (9) (including L_1 and L_2 by using (A3)) and converted into Y^{F1} and Y^{F2} using matrix transformations.
- 5) The diplexer admittance matrix shall be calculated using (4) and (A1) of the appendix, and the S -parameters with (10).

Two examples of diplexer network design are now discussed. The specifications are for typical Rx/Tx for Telecommunication satellites in Ku band and given in Table 1 and Table 3.

Table 1. RF specification example 1.

	Filter 1 (Tx)	Filter 2 (Rx)
Order	5	4
Frequency Bands	12.5–12.75 [GHz]	14–14.25 [GHz]
Return Loss	> -20 [dB]	> -20 [dB]

After running the program, the network results are summarized as follows in Table 2 (a return loss of 25 dB is assumed):

Table 2. Network analysis results.

	Filter 1 (Tx)	Filter 2 (Rx)
f_0	12.625 [GHz]	14.125 [GHz]
$L_{1,2}$	3.46 [mm]	2.12 [mm]
Inverters	0.252768 ($K_{0,1} = K_{5,6}$)	0.231325 ($K_{0,1} = K_{4,5}$)
	0.049528 ($K_{1,2} = K_{4,5}$)	0.041959 ($K_{1,2} = K_{3,4}$)
	0.034711 ($K_{2,3} = K_{4,5}$)	0.031100 ($K_{2,3}$)

The S -parameters calculated are shown in Figure 5. The matching on both channels and the excellent diplexer response can be observed. This model did not require any optimization at network level, resulting in a computation time of just few seconds.

The second example of diplexer design considers a bandwidth of 750 MHz for the first filter and 500 MHz for the second one as indicated in Table 3.

Table 3. RF specification example 2.

	Filter 1 (Tx)	Filter 2 (Rx)
Order	12	10
Frequency Bands	10.95–11.7 [GHz]	14–14.5 [GHz]
Return Loss	> -20 [dB]	> -20 [dB]

Table 4. Network analysis results.

	Filter 1 (Tx)	Filter 2 (Rx)
f_0	11.325 [GHz]	14.25 [GHz]
$L_{1,2}$	3.22 [mm]	1.79 [mm]
Inverters	0.482308 ($K_{0,1} = K_{12,13}$)	0.304014 ($K_{0,1} = K_{10,11}$)
	0.178933 ($K_{1,2} = K_{11,12}$)	0.071112 ($K_{1,2} = K_{3,4}$)
	0.121689 ($K_{2,3} = K_{10,11}$)	0.048402 ($K_{2,3}$)
	0.111251 ($K_{3,4} = K_{9,10}$)	0.044324 ($K_{3,4} = K_{10,11}$)
	0.107722 ($K_{4,5} = K_{8,9}$)	0.043047 ($K_{3,4} = K_{10,11}$)
	0.106329 ($K_{5,6} = K_{7,8}$)	0.042726 ($K_{5,6}$)
	0.105946 ($K_{6,7}$)	—

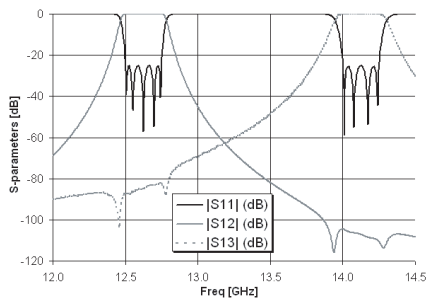


Figure 5. Network S -parameters response of the Diplexer (5 and 4 pole filters).

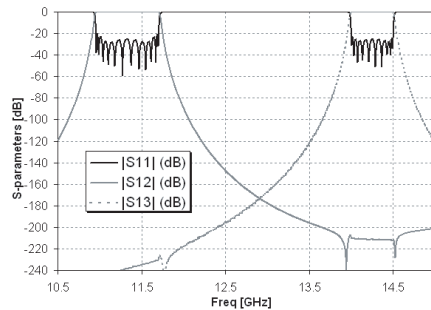


Figure 6. Network S -parameters response of the Diplexer (12 and 10 pole filters).

After running the program, the network results are summarized as follows in Table 4.

The S -parameters calculated are shown in Figure 6. It can be observed the matching on both channels and the excellent diplexer response. The return loss is better than 20 dB on both channels.

In conclusion, the S -parameter results show good performance of the presented network model. The FORTRAN program calculates the S -parameters in few seconds for both cases. This permits to easily predict the performance of diplexers.

4. EXAMPLE OF DIPLEXERS IN RECTANGULAR WAVEGUIDE

A simple and reliable automatic diplexer design procedure has been described for non-contiguous diplexers, substantially reducing the overall computational time from the RF specifications to the final dimensions [5]. This procedure resulted in a FORTRAN code able to assist engineers in diplexer modeling. The procedure ensures fast optimization by the appropriate choice of only six dimensions to be adjusted. Electromagnetic simulations are run with a limited number of variables independent of the filter order.

The software code was run for the two examples previously described. The dimensions found for the first diplexer are reproduced in Table 5. The second structure is given in Table 6. For both cases, WR75 was used and the iris thickness I is 1 mm (see Figure 3(a)). The mathematical computation took less than five minutes.

Table 5. Dimensions of the Diplexer [mm].

	Filter 1 (Tx)	Filter 2 (Rx)
<i>WG type</i>	WR75	WR75
<i>Iris length</i>	1	1
<i>L_{1,2}</i>	1.855	0.908
<i>Resonator lengths</i>	Resonator 1 13.300	Resonator 1 11.237
	Resonator 2 and 4 14.460	Resonator 2 and 3 12.206
	Resonator 3 14.554	Resonator 4 11.251
	Resonator 5 13.260	—
	<i>Iris widths</i>	Iris 1 8.027 Iris 2 and 5 4.583 Iris 3 and 4 4.076 Iris 6 7.989

Table 6. Dimensions of the Diplexer [mm].

<i>WG type</i>	Filter 1 (Tx)	Filter 2 (Rx)
	WR75	WR75
<i>Iris length</i>	1	1
$L_{1,2}$	0.282	0.237
<i>Resonator lengths</i>	Resonator 1 14.110	Resonator 1 10.766
	Resonator 2 and 11 16.174	Resonator 2 and 9 11.811
	Resonator 3 and 10 16.612	Resonator 3 and 8 11.951
	Resonator 4 and 9 16.705	Resonator 4 and 7 11.979
	Resonator 5 and 8 16.738	Resonator 5 and 6 11.988
	Resonator 6 and 7 16.750	Resonator 10 10.660
	Resonator 12 14.090	—
<i>Iris widths</i>	Iris 1 10.744	Iris 1 7.924
	Iris 2 and 12 7.652	Iris 2 and 10 4.801
	Iris 3 and 11 6.714	Iris 3 and 9 4.232
	Iris 4 and 10 6.506	Iris 4 and 8 4.112
	Iris 5 and 9 6.430	Iris 5 and 7 4.073
	Iris 6 and 8 6.407	Iris 6 4.063
	Iris 7 6.399	Iris 11 7.906
Iris 13 11.003	—	

The *S*-parameters of the diplexer analyzed with a fullwave simulator [9] are given in Figure 7. The response shows a return loss better than 20 dB, however this is not equal ripple. This limitation is linked to the dimensional synthesis of the filters themselves and not to the design methodology of the diplexer (i.e., to the choice of the dimensions to adjust via optimization). The limitation of the filter synthesis is linked to the network model which uses frequency independent couplings. An optimization of the individual filter can be useful to achieve equal-ripple performance before finalizing the

diplexer design process. In these specific cases, it was preferred to leave the dimensions as they came directly from the synthesis without any optimization at diplexer (nor filter) level to demonstrate the capability of the design procedure and possible limits.

The S -parameters of the structure analyzed with a fullwave simulator [9] are given in Figure 8. The return loss is better than 18 dB on the first channel and better than 20 dB on the second one. Also in this case the limitation on the achieved return loss is due to the initial fullwave response of the TX filter.

Figure 9 shows the field analysis of the diplexer of Figure 8 at the center frequency of the TX channel ($f = 11.325$ GHz). It can be noted that the electric field is maximum in the TX channel and minimum in the RX channel as expected.

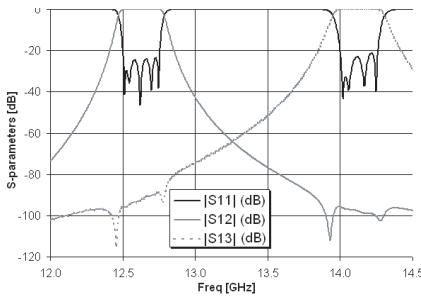


Figure 7. Fullwave response of the Diplexer (5 and 4 pole filters).

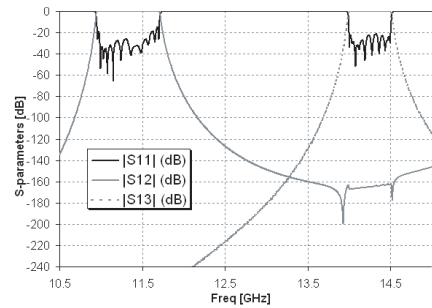


Figure 8. Fullwave response of the Diplexer (12 and 10 pole filters).



Figure 9. Field analysis at the center frequency of the TX channel ($f = 11.325$ GHz).

5. APPLICABILITY OF THE METHOD

The presented computer-aided design of Y-junction waveguide diplexers is limited to the case of non contiguous diplexers, meaning that the rejection provided by the TX channel to the RX channel and opposite is sufficiently high (< 50 dB). Depending on the filter, this is often achieved if the guard-band is in the order of the bandwidth of the wider channel. Note that this has to include any additional spurious that can possibly fall in the second channel.

This is because the impedance inverters as calculated in this paper are based on doubly terminated networks. It is also possible to design a contiguous diplexer using the same procedure but with appropriate couplings based on singly-terminated filters. However, the quality of the synthesis depends on guard-band and the filter types chosen. Therefore optimization of the diplexer is typically necessary to achieve the specified RF performance.

Note that diplexer design and utilization depends upon the applicability range of the waveguide. In any case the entire diplexer band (both channels) has to fall within the applicability range of the waveguide; in the described examples WR75.

6. CONCLUSIONS

A software tool has been developed to support engineers in the design of non-contiguous diplexers using waveguide Y-junctions. The software calculates a mathematical model of the diplexer and can be used for example in establishing the filter order of each frequency band. Examples of designs have been given showing adequate return loss matching of each filter. This model and the equation provided are generic and can be used also for any other junction type by just using another admittance junction matrix.

The software code written in FORTRAN calculates the diplexer dimensions using a procedure already presented by some of the authors and validated with measurements [5]. The use of the mathematical model, supported with automatic dimensional synthesis procedures, allows fast analysis and assessments. This can lead to quick corrections simply by reiterating automatic designs. The applicability and limits of the method are also discussed.

The FORTRAN software code can be further improved allowing diplexer designs using other junction and filter types, but using the same basic approach and formulas as given in the paper.

APPENDIX A.

The Diplexer admittance matrix Y^{Dip} (4) is given analytically using the following expressions:

$$\left\{ \begin{array}{l} Y_{11}^{Dip} = Y_{11} - \frac{+Y_{11}^{F2}Y_{12}Y_{21} + Y_{13}(Y_{11}^{F1} + Y_{22})Y_{31} - Y_{12}Y_{23}Y_{31} - Y_{13}Y_{21}Y_{32} + Y_{12}Y_{21}Y_{33}}{-Y_{23}Y_{32} + (Y_{11}^{F1} + Y_{22})(Y_{11}^{F2} + Y_{33})} \\ Y_{12}^{Dip} = -\frac{Y_{12}^{F1}(Y_{11}^{F2}Y_{12} - Y_{13}Y_{32} + Y_{12}Y_{33})}{Y_{11}^{F2}Y_{22} - Y_{23}Y_{32} + Y_{22}Y_{33} + Y_{11}^{F1}(Y_{11}^{F2} + Y_{33})} \\ Y_{13}^{Dip} = -\frac{Y_{12}^{F2}(Y_{11}^{F1}Y_{13} + Y_{13}Y_{22} - Y_{12}Y_{23})}{Y_{11}^{F2}Y_{22} - Y_{23}Y_{32} + Y_{22}Y_{33} + Y_{11}^{F1}(Y_{11}^{F2} + Y_{33})} \\ Y_{21}^{Dip} = -\frac{Y_{12}^{F1}(-Y_{11}^{F2}Y_{21} + Y_{23}Y_{31} - Y_{21}Y_{33})}{Y_{11}^{F2}Y_{22} - Y_{23}Y_{32} + Y_{22}Y_{33} + Y_{11}^{F1}(Y_{11}^{F2} + Y_{33})} \\ Y_{22}^{Dip} = Y_{22}^{F1} - \frac{(Y_{12}^{F1})^2(Y_{11}^{F2} + Y_{33})}{Y_{11}^{F2}Y_{22} - Y_{23}Y_{32} + Y_{22}Y_{33} + Y_{11}^{F1}(Y_{11}^{F2} + Y_{33})} \\ Y_{23}^{Dip} = \frac{Y_{12}^{F1}Y_{12}^{F2}Y_{23}}{Y_{11}^{F2}Y_{22} - Y_{23}Y_{32} + Y_{22}Y_{33} + Y_{11}^{F1}(Y_{11}^{F2} + Y_{33})} \\ Y_{31}^{Dip} = \frac{Y_{12}^{F2}(-Y_{11}^{F1}Y_{31} - Y_{22}Y_{31} + Y_{21}Y_{32})}{Y_{11}^{F2}Y_{22} - Y_{23}Y_{32} + Y_{22}Y_{33} + Y_{11}^{F1}(Y_{11}^{F2} + Y_{33})} \\ Y_{32}^{Dip} = \frac{Y_{12}^{F1}Y_{12}^{F2}Y_{32}}{Y_{11}^{F2}Y_{22} - Y_{23}Y_{32} + Y_{22}Y_{33} + Y_{11}^{F1}(Y_{11}^{F2} + Y_{33})} \\ Y_{33}^{Dip} = Y_{22}^{F2} - \frac{(Y_{12}^{F2})^2(Y_{11}^{F1} + Y_{22})}{Y_{11}^{F2}Y_{22} - Y_{23}Y_{32} + Y_{22}Y_{33} + Y_{11}^{F1}(Y_{11}^{F2} + Y_{33})} \end{array} \right. \quad (A1)$$

In case impedance matrices Z are used, the following expression is valid:

$$\left\{ \begin{array}{l} Z_{11}^{Dip} = Z_{11} - \frac{+Z_{11}^{F2}Z_{12}Z_{21} + Z_{13}(Z_{11}^{F1} + Z_{22})Z_{31} - Z_{12}Z_{23}Z_{31} - Z_{13}Z_{21}Z_{32} + Z_{12}Z_{21}Z_{33}}{-Z_{23}Z_{32} + (Z_{11}^{F1} + Z_{22})(Z_{11}^{F2} + Z_{33})} \\ Z_{12}^{Dip} = \frac{Z_{12}^{F1}(Z_{11}^{F2}Z_{12} - Z_{13}Z_{32} + Z_{12}Z_{33})}{Z_{11}^{F2}Z_{22} - Z_{23}Z_{32} + Z_{22}Z_{33} + Z_{11}^{F1}(Z_{11}^{F2} + Z_{33})} \\ Z_{13}^{Dip} = \frac{Z_{12}^{F2}(Z_{11}^{F1}Z_{13} + Z_{13}Z_{22} - Z_{12}Z_{23})}{Z_{11}^{F2}Z_{22} - Z_{23}Z_{32} + Z_{22}Z_{33} + Z_{11}^{F1}(Z_{11}^{F2} + Z_{33})} \\ Z_{21}^{Dip} = \frac{Z_{21}^{F1}(Z_{11}^{F2}Z_{21} - Z_{23}Z_{31} + Z_{21}Z_{33})}{Z_{11}^{F2}Z_{22} - Z_{23}Z_{32} + Z_{22}Z_{33} + Z_{11}^{F1}(Z_{11}^{F2} + Z_{33})} \\ Z_{22}^{Dip} = Z_{22}^{F1} - \frac{Z_{12}^{F1}Z_{21}^{F1}(Z_{11}^{F2} + Z_{33})}{Z_{11}^{F2}Z_{22} - Z_{23}Z_{32} + Z_{22}Z_{33} + Z_{11}^{F1}(Z_{11}^{F2} + Z_{33})} \\ Z_{23}^{Dip} = \frac{Z_{12}^{F2}Z_{21}^{F1}Z_{23}}{Z_{11}^{F2}Z_{22} - Z_{23}Z_{32} + Z_{22}Z_{33} + Z_{11}^{F1}(Z_{11}^{F2} + Z_{33})} \\ Z_{31}^{Dip} = -\frac{Z_{21}^{F2}(Z_{11}^{F1}Z_{31} + Z_{22}Z_{31} - Z_{21}Z_{32})}{Z_{23}Z_{32} - (Z_{11}^{F1} + Z_{22})(Z_{11}^{F2} + Z_{33})} \\ Z_{32}^{Dip} = -\frac{Z_{12}^{F1}Z_{21}^{F2}Z_{32}}{Z_{23}Z_{32} - (Z_{11}^{F1} + Z_{22})(Z_{11}^{F2} + Z_{33})} \\ Z_{33}^{Dip} = Z_{22}^{F2} + \frac{Z_{12}^{F2}Z_{21}^{F2}(Z_{11}^{F1} + Z_{22})}{Z_{23}Z_{32} - (Z_{11}^{F1} + Z_{22})(Z_{11}^{F2} + Z_{33})} \end{array} \right. \quad (A2)$$

L_1 and L_2 have to be calculated alternatively using the formula (A3). As indicated in [8], and repeated for simplicity, it is always possible to minimize the reflectivity of the two-port junction realized by closing an arm of a reciprocal and lossless three-port junction, say port 2, on a reactive load jX , provided that the load is position at a distance L :

$$L(f) = \frac{\psi - \phi}{2\beta} \quad (\text{A3})$$

where $e^{j\psi}$ is the reflection of the reactive load, β the propagation constant of the feed waveguides and ϕ is a quantity that depends on the scattering parameters of the junction.

Using the property of the Y-junction $S_{11} = S_{22} = S_{33}$, the formulas given in [8], reduces to the form:

$$\phi = 2 \tan^{-1} \left(\frac{-b + \sqrt{a^2 + b^2 - c}}{c - a} \right) \quad (\text{A4})$$

where

$$\begin{aligned} a &= (1 + a_{11}^2) \sin(\phi_s - 2\phi_{11}) - 2a_{11} \sin(\phi_{11}) \\ b &= (1 + a_{11}^2) \cos(\phi_s - 2\phi_{11}) - 2a_{11} \cos(\phi_{11}) \\ c &= 2a_{11} \sin(3\phi_{11} - \phi_s) \end{aligned}$$

with,

$$\phi_s = \angle (S_{11}^3 - 3S_{11}S_{12}^2 + 2S_{12}^3)$$

In (A4), $S_{11} = a_{11}e^{j\phi_{11}}$ and $S_{12} = a_{12}e^{j\phi_{12}}$ are the scattering parameter at the input port and ϕ_s is the phase of the determinant of the scattering matrix of the three-port junction computed at the frequency f (i.e., alternatively the center frequency of channel one and two). If L is negative then it is necessary to add $\lambda_g/2$.

REFERENCES

1. Cohn, S. B., "Direct-coupled-resonator filters," *Proc. IRE*, Vol. 45, 187–196, Feb. 1957.
2. Levy, R., "Theory of direct coupled cavity filters," *IEEE Trans. on Microwave Theory and Techniques*, Vol. 11, 340–348, Jun. 1967.
3. Rhodes, J. D. and R. Levy, "A generalized multiplexer theory," *IEEE Trans. on Microwave Theory and Techniques*, Vol. 27, 99–111, Feb. 1979.
4. Vanin, F. M., D. Schmitt, and R. Levy, "Dimensional synthesis of wideband waveguide filters," *2004 IEEE MTT-S Symposium Digest*, Vol. 2, 463–466, Jun. 2004.

5. Vanin, F. M., D. Schmitt, and R. Levy, "Dimensional synthesis of wideband waveguide filters and diplexers," *IEEE Trans. on Microwave Theory and Techniques*, Vol. 52, No. 11, 2488–2495, Nov. 2004.
6. Cameron, R. J., R. R. Mansour, and C. M. Kudsia, *Microwave Filters for Communication Systems: Fundamentals, Design and Applications*, Hardcover, Jul. 27, 2007.
7. Matthaei, G. L., L. Young, and E. M. T. Jones, *Microwave Filters, Impedance-matching Networks and Coupling Structures*, McGraw-Hill, New York, 1964.
8. Morini, A., T. Rozzi, and M. Morelli, "New formulae for the initial design in the optimization of T-junction manifold multiplexers," *1997 IEEE MTT-S International Microwave Symposium Digest*, Vol. 2, 1025–1028, Jun. 1997.
9. FEST3D, "Fullwave electromagnetic simulation tool," www.fest3d.com.